

Solubilities of styrene-based polymers and copolymers in common solvents

Oliver Pfohl*, Toshiaki Hino and John M. Prausnitz†

Department of Chemical Engineering, University of California, Berkeley, and Chemical Sciences Division, Lawrence Berkeley Laboratory, Berkeley, CA 94720, USA

(Received 29 August 1994)

A thermo-optical analysis technique is used to obtain cloud-point curves of binary monodisperse polymer/solvent systems containing polystyrene (PS), poly(α -methylstyrene) (PMS) and poly(styrene-*co*- α -methylstyrene) (PSMS) random copolymer having 20 mol% styrene. Solvents include cyclohexane, cyclopentane, *trans*-decalin, *n*-butyl acetate, *n*-pentyl acetate and *n*-hexyl acetate. The systems studied in this work exhibit both a lower critical solution temperature (*LCST*) and an upper critical solution temperature (*UCST*) in the temperature range -60 to 300°C with complete miscibility between *LCST* and *UCST*; exceptions are *trans*-decalin solutions and systems PS/*n*-alkyl acetate which show only *UCST* and *LCST* behaviour, respectively. For systems PMS/*n*-alkyl acetate, PMS/*n*-butyl acetate has the lowest *UCST* while the *LCST* monotonically increases as the molecular weight of *n*-alkyl acetate rises. The critical temperatures of PSMS solutions deviate from the temperature obtained by linearly interpolating between the critical temperature of PS solutions and that of PMS solutions.

(Keywords: styrene-based polymers; solubility; styrene-based copolymers)

INTRODUCTION

In a temperature–composition diagram, many binary polymer solutions exhibit both an upper critical solution temperature (*UCST*) and a lower critical solution temperature (*LCST*) with complete miscibility between *UCST* and *LCST*^{1–4}. In polymer/solvent systems with good solvents, intermolecular interactions are energetically unfavourable in the absence of specific interactions such as hydrogen bonding. The mixture therefore exhibits *UCST* type phase behaviour at low temperature where the energetic effect is dominant. Miscibility above the *UCST* occurs because the entropy of mixing, which favours mutual miscibility, starts to dominate over the energetic effect as the temperature exceeds the *UCST*. At further elevated temperature, however, the equation-of-state effect becomes dominant and the mixture again exhibits phase separation. The equation-of-state effect results from the compressibility disparity between the two components in the mixture; this disparity favours phase separation⁵. For polymer solutions, the compressibility disparity is mainly caused by the difference in molecular sizes.

A fundamental question in polymer solution thermodynamics is how the solubility of a homopolymer changes if an element of repeat unit is replaced by a particular functional group. For copolymer solutions, it is of interest to examine the copolymer-composition dependence of the copolymer's solubility. In this work we report cloud-

point curves of binary monodisperse polymer/solvent systems containing polystyrene, poly(α -methylstyrene) and poly(styrene-*co*- α -methylstyrene) random copolymer having 20 mol% styrene. The six solvents used are cyclohexane, cyclopentane, *trans*-decalin, *n*-butyl acetate, *n*-pentyl acetate and *n*-hexyl acetate. Cloud-point curves were obtained using the thermo-optical analysis (TOA) apparatus described by Bae *et al.*⁴ and by Saraiva *et al.*⁶. The TOA apparatus requires only a very small amount of sample (0.02 – 0.1 cm^3) and yields rapid measurements.

EXPERIMENTAL

Materials and sample preparation

Table 1 gives the weight-average molecular weight, M_w , and the polydispersity factor for each polymer sample. Cyclohexane was obtained from Fisher Scientific (Pittsburgh, PA, USA) and all other solvents were from Aldrich Chemical (Milwaukee, WI, USA). Solvents (purity 99%) were used without further purification.

A polymer solution of known concentration ($\sim 0.5\text{ g}$) was stirred in a vial for at least 8 h. The solution was then introduced into a bottom-sealed quartz glass tube (i.d. = 1 mm, o.d. = 3 mm; GM Associates, Oakland, CA, USA) using a syringe. The system therefore needs to be miscible at room temperature where the sample tube is filled with solution. The top of the sample tube was then sealed at atmospheric pressure using a flame while keeping the sample tube in liquid nitrogen to prevent evaporation of solvent. The pressure inside the sample tube therefore will be near atmospheric at low temperature and close to the vapour pressure of the solvent at elevated temperature.

* Present address: Technische Universität Hamburg-Harburg, Arbeitsbereich Thermische Verfahrenstechnik, Eissendorfer Strasse 38, 21073 Hamburg, Germany

† To whom correspondence should be addressed

Table 1 Characterizations of polymer samples used

Sample designation	Polymer type	Styrene content (mol%)	Mol. wt. (M_w)	M_w/M_n
PS90	Polystyrene ^a	100	90 000	1.04
PS233	Polystyrene ^b	100	233 000	1.06
PS600	Polystyrene ^b	100	600 000	1.10
PS1971	Polystyrene ^c	100	1 971 000	1.26
PMS29	Poly(α -methylstyrene) ^b	0	29 000	1.16
PMS31	Poly(α -methylstyrene) ^b	0	31 200	1.20
PMS61	Poly(α -methylstyrene) ^b	0	61 400	1.05
PMS76	Poly(α -methylstyrene) ^b	0	76 500	1.10
PMS289	Poly(α -methylstyrene) ^b	0	289 000	NA
PSMS114	Poly(styrene- <i>co</i> - α -methylstyrene) random copolymer ^c	20	114 000	1.14

M_n , number-average molecular weight (g mol^{-1})

M_w , weight-average molecular weight (g mol^{-1})

NA, not available

^a Polysciences

^b Pressure Chemical

^c Scientific Polymer

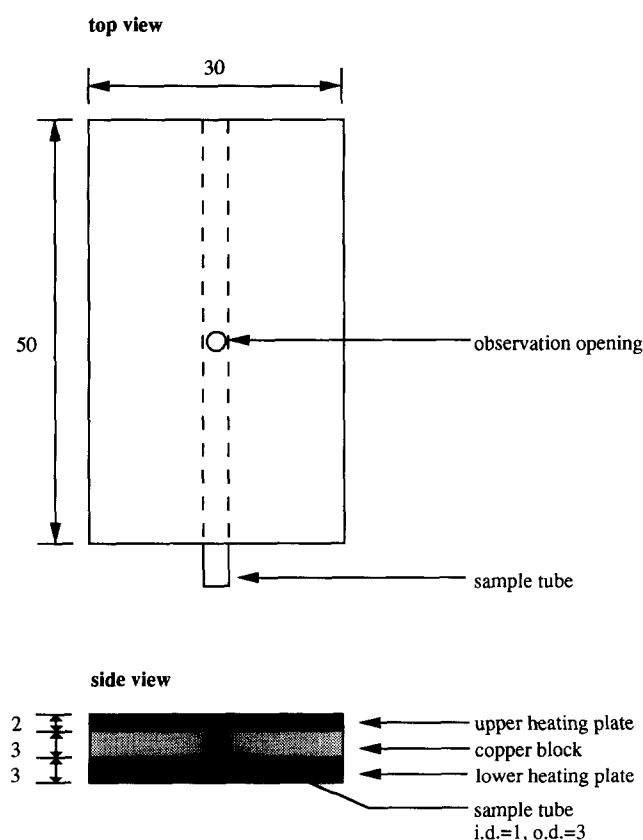


Figure 1 Schematic representation of heating chamber in Mettler FP82 Microscope Hotstage with two copper blocks and a sample tube. All dimensions are in millimetres

The cloud-point temperatures reported here are the averages of measurements for two to four different sample tubes. The standard deviation of measurements for different sample tubes is $\sim 1^\circ\text{C}$ except for the *trans*-decalin solutions ($\sim 2.0^\circ\text{C}$) and for the measurement of the UCST branch in the system PSMS114/*n*-pentyl acetate ($\sim 3^\circ\text{C}$). The relatively large standard deviation

in the UCST branch of the system PSMS114/*n*-pentyl acetate is probably due to an error in concentration because in this system cloud-point temperatures are only slightly higher than the room temperature where samples are prepared.

Apparatus

The TOA apparatus consists of a Mettler Thermo-system (Mettler-Toledo AG, Switzerland) as described by Bae *et al.*⁴ and by Saraiva *et al.*⁶. Using the Mettler FP82 heating-cooling microscope stage, temperatures between -60 and 375°C are attainable. The sample tube is placed between the horizontal heating plates as shown in Figure 1. The additional copper blocks are placed between the heating plates to ensure uniform temperature in the heating chamber⁷. In this work, a one-pound (454 g) weight was placed on the lid of the FP82 hostage to achieve good contact between heating plates, copper blocks and sample tube. In addition, a video camera was attached to the microscope to allow visual inspection of the sample through a monitor. For measurements below room temperature, the apparatus was placed in a box filled with dry nitrogen to prevent condensation of water on the heating-cooling microscope stage.

Procedure

The cloud-point temperature is that temperature at which the first sign of phase separation is detected either by the measured intensity of transmitted light or by visual inspection through a video camera. For the dilute solutions ($< \sim 3 \text{ wt}\%$) studied in this work, visual inspection of sample provides more accurate determination of cloud-point temperatures because these systems did not show a sharp decrease in the measured intensity of transmitted light. In most of the systems that show a sharp decrease in the measured intensity of transmitted light, the cloud-point temperature determined by the intensity measurement agrees with the cloud-point temperature determined by visual inspection to within 0.1°C .

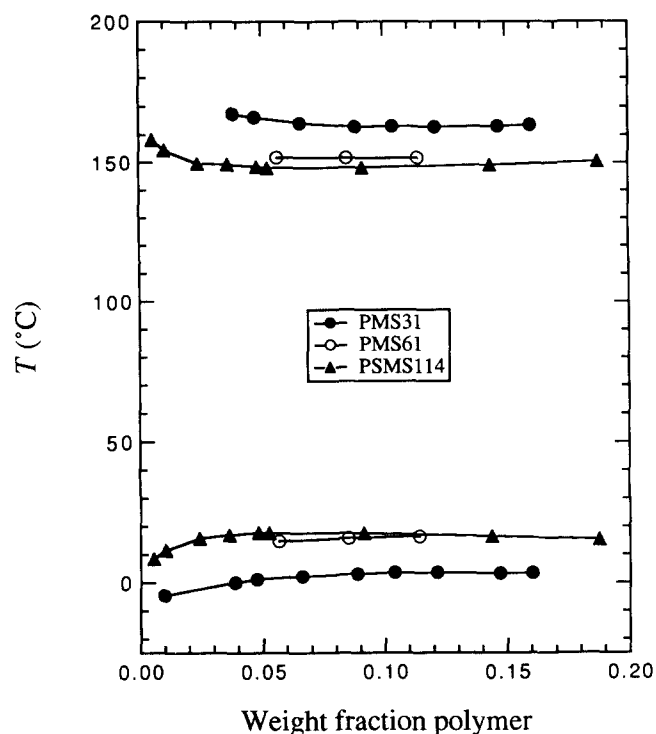


Figure 2 Cloud-point curves for the systems poly(α -methylstyrene)/cyclopentane and poly(styrene-*co*- α -methylstyrene)/cyclopentane. Cloud-point data are given in Table 2

The cloud-point temperatures of *LCST* and *UCST* branches were determined upon heating and cooling, respectively, with the heating and cooling rate of 1°C min^{-1} , except for the system with PS1971 ($0.1^\circ\text{C min}^{-1}$) and for the measurement of the *LCST* branch in the system PMS614/cyclohexane (3°C min^{-1}). A higher heating rate was used in the system PMS614/cyclohexane to avoid the effect of superheating which, in this system, was about 10°C . For other systems, the effect of supercooling or superheating⁴ was less than 0.5°C .

An elementary heat-transfer analysis⁸ reveals that for a finite heating and cooling rate of $Q \text{ min}^{-1}$ (where Q is measured in $^\circ\text{C}$), the difference between the thermometer reading and the temperature of the sample is approximately $0.3Q$. At various heating rates, the measurements of nematic-isotropic phase-transition temperatures (T_{NI}) of 4,4'-di-methoxyazoxybenzene (a liquid crystal) by Pfohl *et al.*⁷ show that the difference between the measured T_{NI} and the true T_{NI} is about $0.3Q$. The data reported here are corrected for the effect of finite heating and cooling rate, $0.3Q$. Depending on the polydispersity of polymer samples, the maximum points of the cloud-point curves deviate slightly from the critical points. Since the polymer samples used here are monodisperse, we report the maximum and the minimum of cloud-point curves as the *UCST* and the *LCST*, respectively.

RESULTS AND DISCUSSION

When comparing the critical temperatures obtained in this work with those in the literature, it is necessary to make a comparison for the same molecular weight of polymer. The critical temperatures for the molecular weights of polymer used in this work can be estimated by the Shultz-Flory plot⁹ using previously measured

critical temperatures of various molecular weights of the same polymer. The Shultz-Flory plot⁹ is given by

$$\frac{1}{T_c} = \frac{1}{\theta} \left\{ 1 + \frac{1}{\psi} \left(\frac{1}{r^{1/2}} + \frac{1}{2r} \right) \right\} \quad (1)$$

where T_c is the critical temperature, θ is the theta temperature, ψ is an entropy parameter and r is the ratio of the molar volume of polymer to the molar volume of solvent. The theta temperature can be identified as the critical temperature for the infinite-molecular-weight polymer when $r \rightarrow \infty$. For the system exhibiting both *UCST* and *LCST*, there are two theta temperatures: the theta temperature associated with the *UCST*, θ_U , and that associated with the *LCST*, θ_L . In the Flory-Huggins theory, the theta temperature associated with *UCST* can also be defined as the temperature at which the osmotic second virial coefficient vanishes.

In this work, the molar volumes of polymer and solvent are calculated using the measured densities. Equation (1) predicts that the plot of $1/T_c$ against $(1/r^{1/2} + 1/2r)$ is a straight line. The measured critical temperatures of various molecular weights of polymer are fitted to equation (1) to obtain θ and ψ . Once θ and ψ are known, equation (1) provides the molecular-weight dependence of the critical temperature.

Figure 2 shows cloud-point curves for the systems poly(α -methylstyrene) (PMS)/cyclopentane and poly(styrene-*co*- α -methylstyrene) (PSMS)/cyclopentane. These phase diagrams are similar to the cloud-point curves for the system polystyrene (PS)/cyclopentane reported by Saeki *et al.*² Table 2 gives experimental cloud-point data for cyclopentane solutions.

Figure 3 shows cloud-point curves for the systems PMS/cyclohexane and PSMS/cyclohexane. In the system PMS/cyclohexane, the *UCSTs* for $M_w = 61\,400$ and

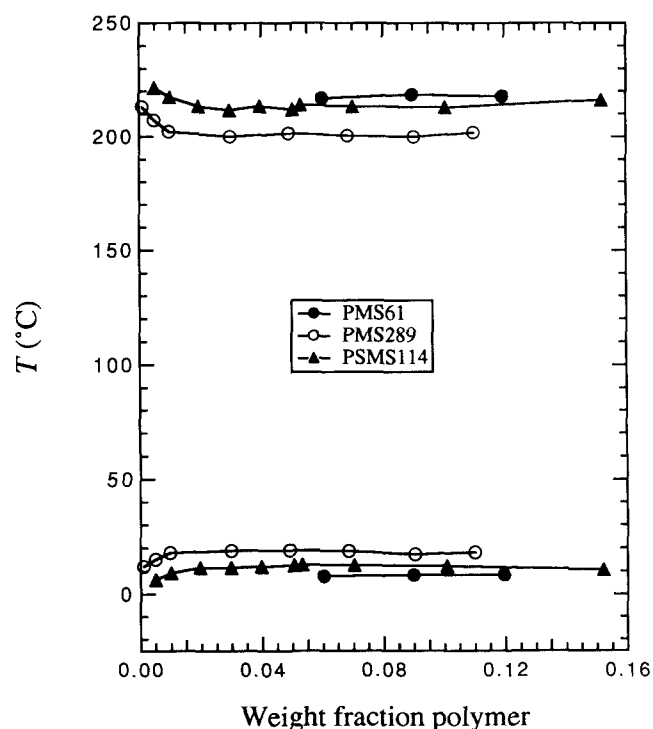


Figure 3 Cloud-point curves for the poly(α -methylstyrene)/cyclohexane systems and for the poly(styrene-*co*- α -methylstyrene)/cyclohexane system. Cloud-point data are given in Table 3

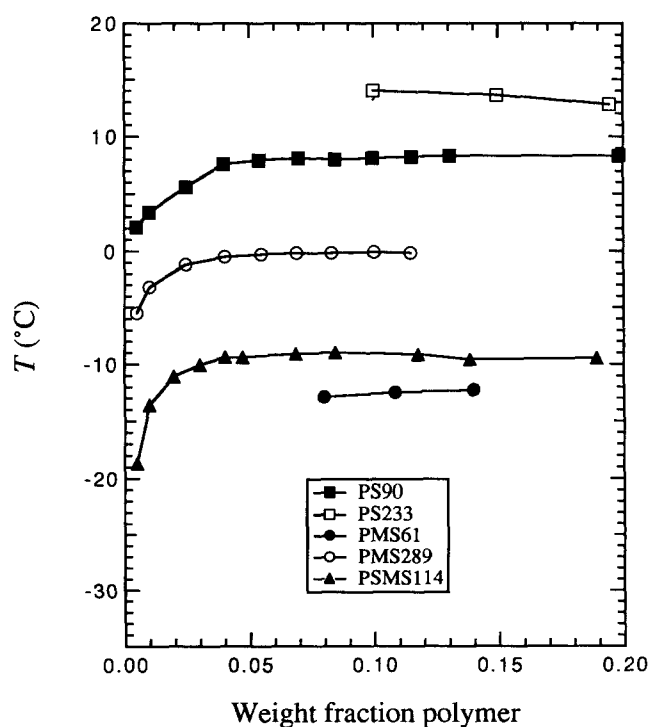
Table 2 Experimental cloud-point data for cyclopentane solutions

PMS31			PMS61			PSMS114		
W_2^a	$T_U(^{\circ}\text{C})$	$T_L(^{\circ}\text{C})$	W_2	$T_U(^{\circ}\text{C})$	$T_L(^{\circ}\text{C})$	W_2	$T_U(^{\circ}\text{C})$	$T_L(^{\circ}\text{C})$
0.0098	-4.7		0.0566	14.8	151.8	0.0053	8.5	158.2
0.0384	-0.1	167.3	0.0850	15.8	151.6	0.0104	11.5	154.4
0.0474	1.1	166.1	0.1141	16.3	151.6	0.0241	15.8	149.5
0.0660	2.1	164.1				0.0364	17.0	149.3
0.0886	2.8	162.8				0.0482	17.8	148.4
0.1038	3.4	163.1				0.0526	17.7	147.9
0.1211	3.5	162.8				0.0913	17.5	148.1
0.1469	3.1	163.1				0.1437	16.5	149.1
0.1601	3.3	163.5				0.1876	15.3	150.2

 T_U , upper consolute temperature T_L , lower consolute temperature^aWeight fraction of polymer**Table 3** Experimental cloud-point data for cyclohexane solutions

PMS61			PMS289			PSMS114		
W_2	$T_U(^{\circ}\text{C})$	$T_L(^{\circ}\text{C})$	W_2	$T_U(^{\circ}\text{C})$	$T_L(^{\circ}\text{C})$	W_2	$T_U(^{\circ}\text{C})$	$T_L(^{\circ}\text{C})$
0.0603	7.7	216.9	0.0010	11.9	213.0	0.0050	6.2	221.5
0.0898	8.1	218.5	0.0050	14.9	207.1	0.0101	9.0	217.4
0.1196	8.4	217.7	0.0097	17.8	202.2	0.0196	11.4	213.3
			0.0299	18.8	200.0	0.0297	11.4	211.7
			0.0491	18.9	201.4	0.0398	11.9	213.4
			0.0685	18.5	200.3	0.0505	12.5	212.0
			0.0904	17.2	199.8	0.0532	12.7	213.9
			0.1100	18.1	201.7	0.0703	12.4	213.2
						0.1008	12.2	212.8
						0.1521	10.4	216.1

For abbreviations, see Table 2

**Figure 4** Cloud-point curves for *trans*-decalin solutions. Cloud-point data are given in Table 4

$M_w = 289\,000$ (8.4 ± 1 and $18.9 \pm 1^{\circ}\text{C}$, respectively) agree with those for the same molecular weights obtained from the Shultz-Flory plot using the data by Volkova *et al.*¹⁰, 8.5 ± 2.5 and $20.5 \pm 1.5^{\circ}\text{C}$, respectively. Volkova *et al.* obtained the molecular-weight dependence of the critical temperature by measuring the critical opalescence. Cloud-point curves for the system PS/cyclohexane are given in ref. 1. Table 3 gives experimental cloud-point data for cyclohexane solutions.

Figure 4 shows cloud-point curves for *trans*-decalin solutions. These systems do not exhibit LCST-type phase behaviour below $\sim 300^{\circ}\text{C}$. Although the critical temperatures were determined only for two different molecular weights of polymer, for the system PS/*trans*-decalin, the theta temperature $23.7 \pm 1^{\circ}\text{C}$ determined from equation (1) with the data obtained in this work shows good agreement with the theta temperatures in the literature^{11–15}. The theta temperature for the system PMS/*trans*-decalin determined from equation (1) with the data obtained in this work is $11.0 \pm 1^{\circ}\text{C}$. For this system, Kato *et al.*¹⁶ also report $\theta_U = 9.5 \pm 0.5^{\circ}\text{C}$, determined by the measurement of second virial coefficients. Figures 3 and 4 show that for a given molecular weight of polymer, the UCST in cyclohexane solutions is higher than that in *trans*-decalin solutions. Table 4 gives experimental cloud-point data for *trans*-decalin solutions.

Table 4 Experimental cloud-point data for *trans*-decalin solutions

PS90		PS233		PMS61		PMS289		PSMS114	
W_2	$T_U(^{\circ}\text{C})$	W_2	$T_U(^{\circ}\text{C})$	W_2	$T_U(^{\circ}\text{C})$	W_2	$T_U(^{\circ}\text{C})$	W_2	$T_U(^{\circ}\text{C})$
0.0049	2.1	0.0999	14.0	0.0799	-12.9	0.0050	-5.5	0.0050	-18.7
0.0099	3.4	0.1494	13.6	0.1084	-12.5	0.0099	-3.2	0.0099	-13.6
0.0247	5.6	0.1947	12.8	0.1399	-12.3	0.0246	-1.2	0.0197	-11.1
0.0398	7.6					0.0403	-0.5	0.0301	-10.1
0.0540	7.9					0.0550	-0.3	0.0402	-9.4
0.0699	8.1					0.0692	-0.2	0.0473	-9.4
0.0847	8.0					0.0831	-0.2	0.0687	-9.1
0.0996	8.1					0.1003	-0.1	0.0845	-9.0
0.1153	8.2					0.1150	-0.2	0.1177	-9.2
0.1306	8.3							0.1385	-9.6
0.1984	8.3							0.1893	-9.5

For abbreviations, see Table 2

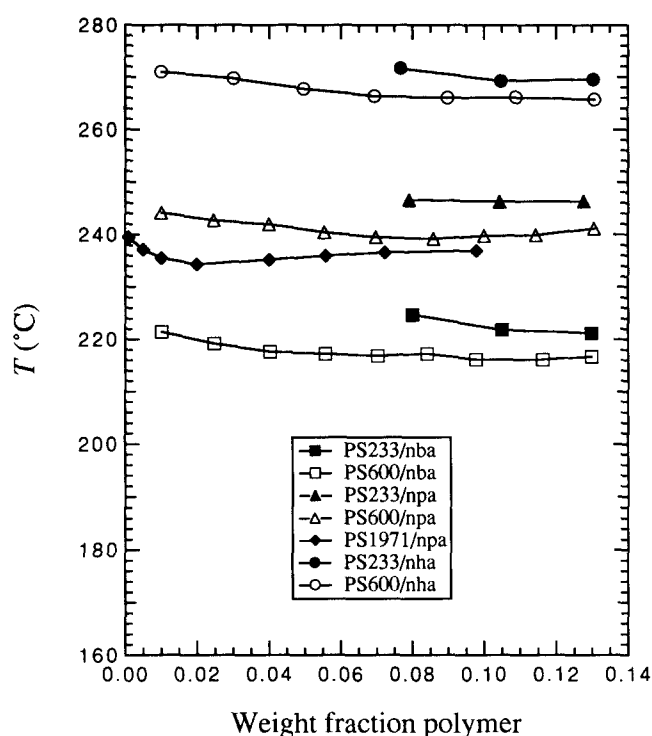
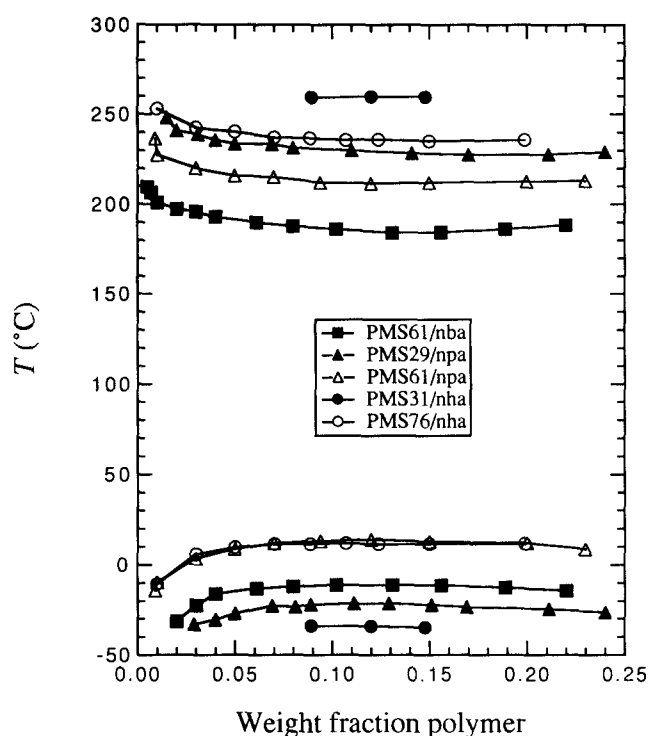
**Figure 5** Cloud-point curves for the system PS/*n*-alkyl acetate (nbs = *n*-butyl acetate; npa = *n*-pentyl acetate; nha = *n*-hexyl acetate). Cloud-point data are given in Table 5

Figure 5 shows cloud-point curves for the system PS/*n*-alkyl acetate. The *LCST* increases as the molecular weight of *n*-alkyl acetate rises. We represent *n*-alkyl acetates by $\text{C}_i\text{H}_{2i+1}\text{COOCH}_3$. The systems shown in Figure 5 do not exhibit *UCST*-type phase behaviour above -50°C . This observation is expected because θ_U for polystyrene solutions in methyl acetate ($i=1$), ethyl acetate ($i=2$), and *n*-propyl acetate ($i=3$) are reported as $+43$, -44 and -80°C , respectively, that is, the *UCST* decreases as the molecular weight of *n*-alkyl acetate rises. Table 5 gives experimental cloud-point data for PS in *n*-alkyl acetates.

Figure 6 shows cloud-point curves for the system PMS/*n*-alkyl acetate exhibiting both *UCST* and *LCST*. The data for the *n*-butyl acetate (nba) and *n*-pentyl acetate

**Figure 6** Cloud-point curves for the system PMS/*n*-alkyl acetate. Data for *n*-butyl acetate and *n*-pentyl acetate solutions are from Bungert¹⁷. Cloud-point data are given in Table 6

(npa) solutions are from Bungert¹⁷. In the molecular-weight range shown in Figure 6, the *UCST* is more sensitive to the molecular weight of PMS than is the *LCST*. Surprisingly, the *UCST* for the system PMS61/nba is lower than those for the systems PMS61/npa and PMS76/nha while the *LCST* for the system PMS61/nba is the lowest. The results shown in Figures 5 and 6 indicate that for a given molecular weight of polymer, the *LCST* in the system PS/*n*-alkyl acetate is higher than that in the system PMS/*n*-alkyl acetate. Conversely, the *UCST* in the system PS/*n*-alkyl acetate is lower than that in the system PMS/*n*-alkyl acetate. PS is therefore more soluble than PMS in *n*-alkyl acetate. Table 6 gives experimental cloud-point data for PMS in *n*-alkyl acetates.

Figures 7 shows cloud-point curves for the system

Table 5 Experimental cloud-point data for polystyrene in n-alkyl acetate

PS233/nba		PS600/nba		PS233/npa		PS600/npa		PS1971/npa		PS233/nha		PS600/nha	
W_2	T_L (°C)	W_2	T_L (°C)	W_2	T_L (°C)	W_2	T_L (°C)	W_2	T_L (°C)	W_2	T_L (°C)	W_2	T_L (°C)
0.0800	224.7	0.0101	221.4	0.0791	246.5	0.0100	244.1	0.0010	239.5	0.0768	271.6	0.0100	270.9
0.1050	221.8	0.0248	219.1	0.1043	246.2	0.0247	242.7	0.0050	237.1	0.1048	269.2	0.0301	269.7
0.1298	221.2	0.0403	217.6	0.1277	246.3	0.0400	241.9	0.0100	235.5	0.1304	269.5	0.0496	267.7
		0.0557	217.2			0.0554	240.4	0.0199	234.3			0.0694	266.3
		0.0703	216.8			0.0698	239.5	0.0400	235.2			0.0898	266.0
		0.0841	217.2			0.0859	239.2	0.0558	236.0			0.1088	266.1
		0.0977	216.1			0.1001	239.7	0.0724	236.6			0.1306	265.7
		0.1163	216.1			0.1144	239.9	0.0979	236.9				
		0.1298	216.6			0.1306	241.1						

nba, n-butyl acetate

npa, n-pentyl acetate

nha, n-hexyl acetate

For definitions of W_2 and T_L , see Table 2**Table 6** Experimental cloud-point data for poly(α -methylstyrene) in n-alkyl acetate

PMS61/nba			PMS29/npa			PMS61/npa			PMS31/nha			PMS76/nha		
W_2	T_U (°C)	T_L (°C)	W_2	T_U (°C)	T_L (°C)	W_2	T_U (°C)	T_L (°C)	W_2	T_U (°C)	T_L (°C)	W_2	T_U (°C)	T_L (°C)
0.005		209.5	0.015		248.1	0.009	-14.4	236.5	0.0894	-34.1	259.1	0.0100	-10.8	253.1
0.007		206.5	0.020		241.0	0.010	-9.8	227.5	0.1200	-34.3	259.7	0.0301	5.6	242.3
0.010		200.9	0.029	-33.1		0.030	3.4	219.9	0.1479	-35.0	259.4	0.0500	9.5	240.2
0.020	-31.4	197.3	0.031		238.7	0.050	8.7	215.8				0.0702	11.4	237.1
0.030	-22.6	195.7	0.040	-30.6	235.6	0.070	11.9	215.2				0.0886	11.3	236.6
0.040	-16.3	193.1	0.050	-27.2	233.6	0.094	12.9	212.0				0.1071	11.9	235.7
0.061	-13.3	189.9	0.069	-22.8	233.3	0.120	13.9	211.5				0.1239	11.3	236.0
0.080	-12.2	187.8	0.080		231.4	0.150	12.8	212.0				0.1499	11.3	235.0
0.102	-11.2	186.1	0.081	-23.5		0.200	12.1	212.5				0.1990	11.6	235.7
0.131	-11.1	184.0	0.089	-22.1		0.230	8.7	213.0						
0.156	-11.4	184.2	0.110		229.9									
0.189	-12.6	186.1	0.111	-21.6										
0.220	-14.4	188.3	0.129	-21.6										
			0.141		228.4									
			0.151	-22.4										
			0.169	-23.5										
			0.170		227.5									
			0.211	-24.6	227.6									
			0.240	-26.5	229.0									

Data for nba and npa solutions are from Bungert¹⁷

For abbreviations, see Tables 2 and 5

PSMS/n-alkyl acetate. Similar to the cloud-point curves for the system PMS/n-alkyl acetate, both the *UCST* and *LCST* for the system PSMS114/nba are lower than those for the system PSMS114/npa. Table 7 gives experimental cloud-point data for PSMS in n-alkyl acetates.

The results obtained here raise a question concerning how the critical temperatures in the systems PS/n-alkyl acetate and PMS/n-alkyl acetate vary with the size of homologous solvent, n-alkyl acetate. In addition to the data for the system PS/n-alkyl acetate obtained in this work, cloud-point curves for various molecular weights of polystyrene in methyl acetate, ethyl acetate and n-propyl acetate are given by Saeki *et al.*³. Using the Shultz-Flory plot, equation (1), it is possible to estimate

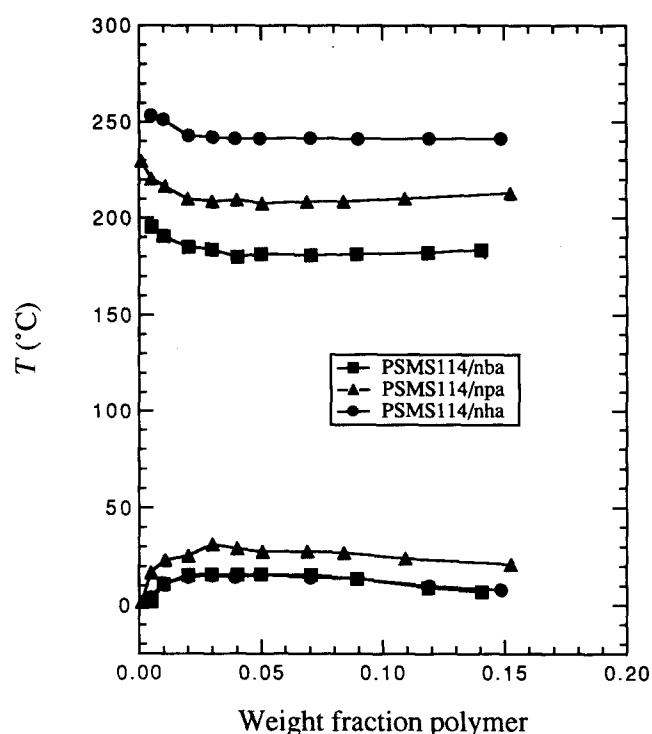
the *LCST* in the systems studied by Saeki *et al.*³ for the molecular weight of PS used in this work.

Figure 8 shows the *LCSTs* in the system PS/n-alkyl acetate for $M_w = 233\,000$, $600\,000$ and $1\,971\,000$. The data for $i = 1$ to 3 are obtained from the Shultz-Flory plot using the data of Saeki *et al.*³. Theta temperatures θ_U for polystyrene solutions in n-alkyl acetate monotonically decrease as the molecular weight of n-alkyl acetate rises from $i = 1$ to 3. The decrease in the *UCST* indicates that interactions between PS and n-alkyl acetate become energetically more favourable as the molecular weight of n-alkyl acetate rises, probably because the acetoxyl group ($\text{CH}_3\text{COO}-$), which has unfavourable interactions with PS, becomes less dominant as the size of the alkyl group

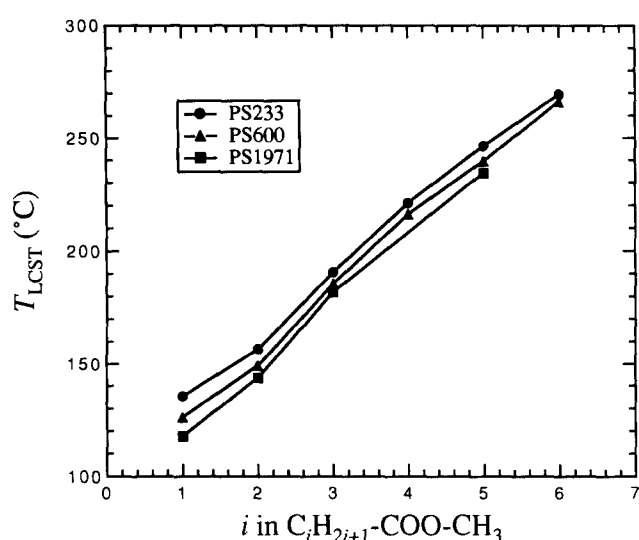
Table 7 Experimental cloud-point data for poly(styrene-co- α -methylstyrene) in n-alkyl acetate

PSMS114/nba			PSMS114/npa			PSMS114/nha		
W_2	$T_U(^{\circ}\text{C})$	$T_L(^{\circ}\text{C})$	W_2	$T_U(^{\circ}\text{C})$	$T_L(^{\circ}\text{C})$	W_2	$T_U(^{\circ}\text{C})$	$T_L(^{\circ}\text{C})$
0.0050	1.7	195.3	0.0010	1.4	229.6	0.0050	3.9	253.4
0.0100	10.5	190.4	0.0050	16.6	220.4	0.0100	11.1	251.0
0.0202	15.2	185.0	0.0107	23.1	216.4	0.0202	14.2	242.7
0.0298	15.6	183.7	0.0201	25.1	209.8	0.0301	15.1	241.9
0.0403	15.5	179.9	0.0301	31.1	208.4	0.0393	14.2	241.4
0.0501	15.7	181.3	0.0401	29.1	209.3	0.0496	15.4	241.3
0.0705	15.4	180.8	0.0505	27.3	207.5	0.0703	14.0	241.5
0.0893	13.6	181.3	0.0689	27.5	208.2	0.0899	13.6	241.1
0.1187	8.8	181.9	0.0840	26.8	208.4	0.1192	9.8	241.3
0.1405	6.8	183.4	0.1093	24.0	209.9	0.1486	7.8	241.0
			0.1527	20.9	212.8			

For abbreviations, see Tables 2 and 5

**Figure 7** Cloud-point curves for the system PSMS/n-alkyl acetate. Cloud-point data are given in Table 7

(C_iH_{2i+1}) increases. The increase in the $LCST$, however, may also be caused by the decreased equation-of-state effect as the ratio of molecular sizes declines. The $LCST$ in Figure 5 is caused by the equation-of-state effect which originates from the disparity in compressibility for the components. For polymer solutions, the compressibility disparity is mainly due to the difference in molecular size. It is therefore to be expected that, for a given molecular weight of polymer, the equation-of-state effect becomes less dominant as the molecular weight of homologous solvent rises, leading to increased solubility of polymer and higher $LCST$. As the molecular weight of homologous solvent rises further, however, the $LCST$ decreases because the entropy of mixing, which favours mutual

**Figure 8** $LCST$ for the system PS/n-alkyl acetate

miscibility, decreases as the size of solvent increases. As the molecular weight of homologous solvent rises, increased $LCST$ is reported for the system polyisobutylene/n-alkanes and polyethylene/n-alkanes¹⁸.

Figure 9 shows $UCSTs$ and $LCSTs$ for the systems PMS/n-alkyl acetate ($M_w=31\,200$ and $61\,400$) and PSMS114/n-alkyl acetate. The critical solution temperatures for $M_w=31\,200$ in n-pentyl acetate and those for $M_w=61\,400$ in n-hexyl acetate are obtained using the Shultz-Flory plot using the data shown in Figure 6. The system PSMS114/n-propyl acetate ($i=3$) is immiscible at room temperature. The $UCST$ for this system was determined by visual inspection using a glass tube (i.d. = 12 mm; o.d. = 14 mm; sample volume $\approx 1\text{ cm}^3$) immersed in a temperature-controlled water bath. The $UCST$ in the system PMS31/n-butyl acetate ($i=4$) lies below -60°C , the lower limit of measurements. The $UCST$ is therefore the lowest in n-butyl acetate ($i=4$) for the system PMS/n-alkyl acetate while the $LCST$ monotonically increases as the molecular weight of n-alkyl acetate rises. The $UCST$ is the lowest for the n-butyl acetate solution, probably because the interaction between PMS and n-butyl acetate is energetically favourable. The

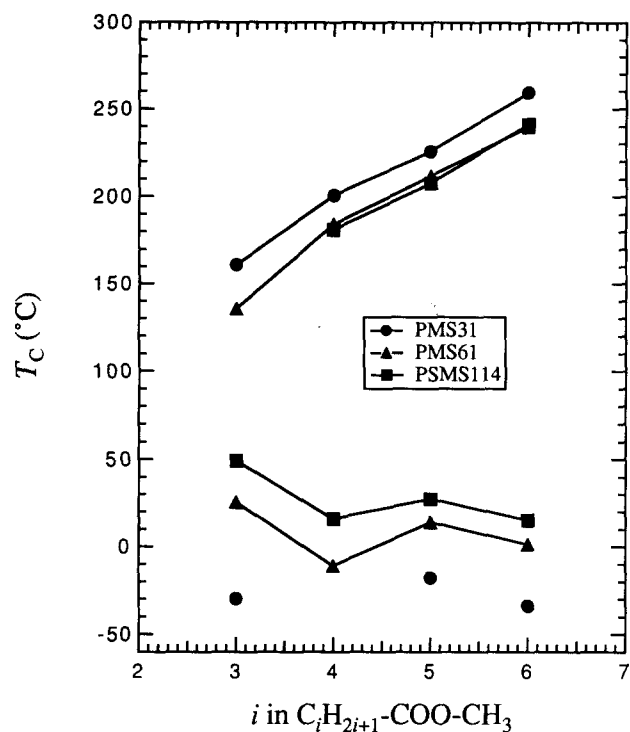


Figure 9 Critical temperatures for the systems PMS/n-alkyl acetate and PSMS/n-alkyl acetate. The *UCST* in n-butyl acetate ($i=4$) lies below -60°C , the lower limit of measurements

Table 8 *UCST* and *LCST* ($^\circ\text{C}$) for $M_w = 114\,000$

Solvent	PMS		PS		PSMS	
	T_{UCST}	T_{LCST}	T_{UCST}	T_{LCST}	T_{UCST}	T_{LCST}
Cyclopentane	25.7	144.6	4.2	170.9	17.8	147.9
Cyclohexane	13.5	208.3	21.4	227.6	12.7	211.7
<i>Trans</i> -decalin	-6.4		10.0		-9.0	
n-Butyl acetate		173.9		227.2	15.7	179.9
n-Pentyl acetate	39.2	202.8		254.5	30.0	207.5
n-Hexyl acetate	30.2	227.9		273.3	15.4	241.0

origin of favourable interaction in this system however, is not obvious.

The energetic effect is dominant at low temperature. At elevated temperature, however, the energetic effect is not strong enough to raise the *LCST* for the n-butyl acetate solution above that for the n-pentyl acetate solution ($i=5$). The *UCST* for the system PSMS114/n-butyl acetate is also lower than that obtained by linearly interpolating between the *UCST* for n-propyl acetate solution ($i=3$) and that for n-pentyl acetate solution ($i=5$).

Solubility of PSMS random copolymer

To determine the copolymer composition dependence of the solubility of PSMS random copolymer, we estimate the *UCST* and *LCST* of PS and PMS solutions for $M_w = 114\,000$ (the molecular weight of PSMS used in this work) using the Shultz-Flory plot with data obtained in this work and literature data. The uncertainty in the critical temperature for $M_w = 114\,000$ obtained in this manner is estimated to be between 1 and 3.5°C if the measured critical temperatures used in the Shultz-Flory

plot have an uncertainty of 1°C ⁸. Table 8 gives *UCST* and *LCST* values for PS, PMS and PSMS solutions for $M_w = 114\,000$.

Figures 10 and 11 show the copolymer-composition dependences of the *UCST* and *LCST*, respectively, for $M_w = 114\,000$. The *UCST* in copolymer solutions is lower than that obtained by linearly interpolating between the *UCSTs* for homopolymer solutions. This observation agrees with the result by Goldwasser and Williams¹⁹ who determined the theta temperature associated with the *UCST* in PSMS solutions. The *UCST* for copolymer solutions can be lower than those for the relevant homopolymer solutions for the following reason²⁰. Let the copolymer solution be designated as $A/(C_Y B_{1-Y})_r$, where A is the solvent molecule, C and B represent the segments that comprise the copolymer, and Y is the mole fraction of segment C in the copolymer. If the interaction between segments C and B of copolymer of type $(C_Y B_{1-Y})_r$ is unfavourable, the intramolecular interaction between copolymers could become more unfavourable as the copolymer composition varies and the intermolecular interaction between copolymer and solvent becomes more favourable relative to copolymer intramolecular interactions, leading to enhanced solubility of copolymers. This enhanced solubility is often called the intramolecular repulsion effect. In that event the *UCST* and *LCST* can be lower and higher, respectively, than those obtained by linearly interpolating between the critical temperatures of relevant homopolymer solutions. The intramolecular repulsion effect is expected to be less apparent near the *LCST* because the energetic effect is less significant at elevated temperatures.

Figure 11 shows that for a given solvent, the *LCST* for a PS solution is 25– 50°C higher than that for a PMS solution. Figure 11 also shows that the *LCST* for a copolymer solution is higher than that obtained by

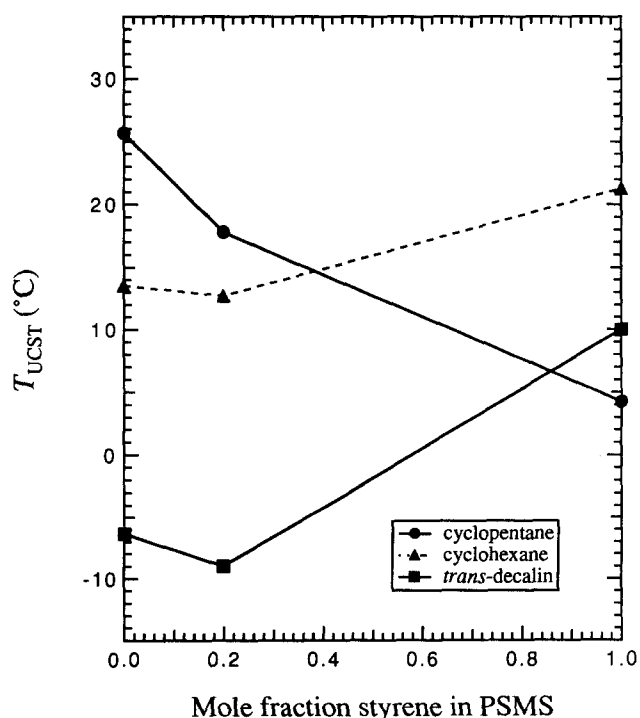


Figure 10 Copolymer-composition dependence of *UCST* for $M_w = 114\,000$. *UCST* values are given in Table 8

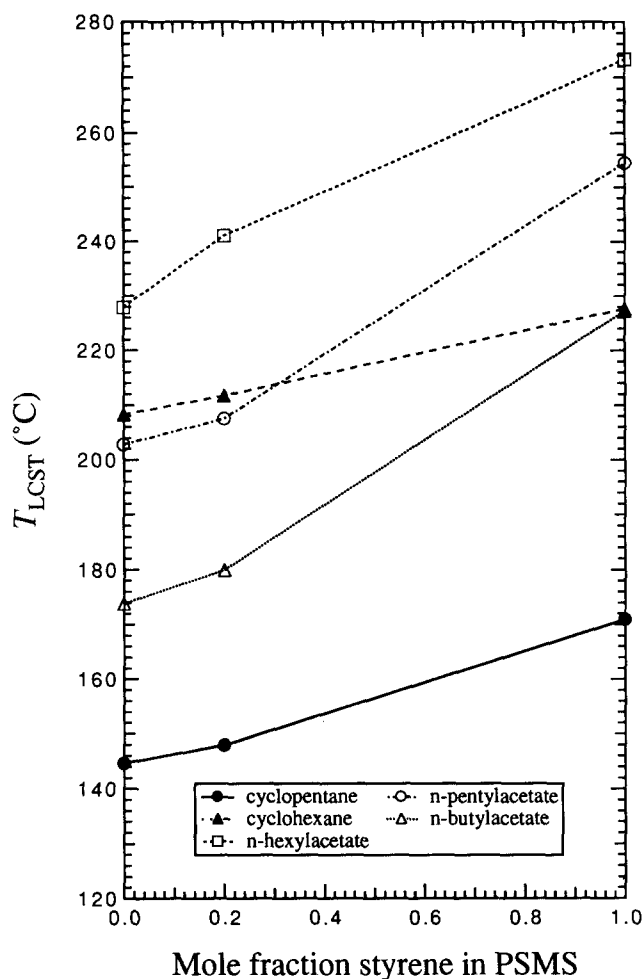


Figure 11 Copolymer-composition dependence of $LCST$ for $M_w = 114\,000$. $LCST$ values are given in Table 8

linearly interpolating between the $LCST$ s for homopolymer solutions in n-hexyl acetate. On the other hand, however, the $LCST$ for a copolymer solution is lower than that obtained by linearly interpolating between the $LCST$ s for homopolymer solutions in cyclopentane, n-pentyl acetate and n-butyl acetate. These results may indicate that the intramolecular repulsion effect is not strong at elevated temperature. To provide meaningful analysis of the copolymer-composition dependence of $LCST$, however, it is necessary to use equation-of-state theories that are capable of predicting the $LCST$ in polymer solutions.

CONCLUSIONS

Cloud-point curves are obtained for binary polymer/solvent systems containing polystyrene (PS), poly(α -methylstyrene) (PMS), and poly(styrene-co- α -methylstyrene) (PSMS) having 20 mol% styrene using a thermo-optical analysis technique. For systems PS/n-alkyl acetate,

the $LCST$ monotonically increases as the molecular weight of solvent rises. For systems PMS/n-alkyl acetate, the system PMS/n-butyl acetate has the lowest $UCST$ while the $LCST$ monotonically increases as the molecular weight of n-alkyl acetate rises. The critical temperature of PSMS solutions deviates from the temperature obtained by linearly interpolating between the critical temperature of PS solutions and that of PMS solutions.

ACKNOWLEDGEMENTS

This work was supported by the Director, Office of Energy Research, Office of Basic Energy Sciences, Chemical Sciences Division of the US Department of Energy under Contract No. DE-AC03-76SF0098. Additional funding was provided by E. I. du Pont de Nemours & Co. (Philadelphia, PA) and Koninklijke Shell (Amsterdam, The Netherlands) and by the Donors of the Petroleum Research Fund administered by the American Chemical Society. For financial support O. Pföhl also thanks the Ernest Solvay Stiftung (Stifterverband für die deutsche Wissenschaft). The authors thank B. Bungert for extensive assistance in experimental work.

REFERENCES

- 1 Saeki, S., Kuwahara, N., Konno, S. and Kaneko, M. *Macromolecules* 1973, **6**, 246
- 2 Saeki, S., Kuwahara, N., Konno, S. and Kaneko, M. *Macromolecules* 1973, **6**, 589
- 3 Saeki, S., Konno, S., Kuwahara, N., Nakata, M. and Kaneko, M. *Macromolecules* 1974, **7**, 521
- 4 Bae, Y. C., Lambert, S. M., Soane, D. S. and Prausnitz, J. M. *Macromolecules* 1991, **24**, 4403
- 5 Patterson, D. *Macromolecules* 1969, **2**, 672
- 6 Saraiva, A., Persson, O. and Fredenslund, A. *Fluid Phase Equilibria* 1993, **91**, 291
- 7 Pföhl, O., Hino, T. and Prausnitz, J. M. *Fluid Phase Equilibria* in press
- 8 Pföhl, O. *Diplomarbeit*, performed at University of California, Berkeley; deposited at Technische Universität Hamburg-Harburg, Arbeitsbereich Thermische Verfahrenstechnik, 1994
- 9 Shultz, A. R. and Flory, P. J. *J. Am. Chem. Soc.* 1952, **74**, 4760
- 10 Volkova, L. A., Andreeva, N. A., Podol'skii, A. F., Taran, A. A. and Eskin, V. E. *Vysokomol. Soed. Ser. A* 1977, **19**, 475
- 11 Schulz, G. V. and Baumann, H. *Makromol. Chem.* 1963, **60**, 120
- 12 Inagaki, H., Suzuki, H., Fujii, M. and Matsuo, T. *J. Phys. Chem.* 1966, **70**, 1718
- 13 Berry, G. C. *J. Chem. Phys.* 1966, **44**, 4550
- 14 Kotera, A., Matsuda, H., Konishi, K. and Takemura, K. *J. Polym. Sci., C* 1968, **23**, 619
- 15 Konno, S., Saeki, S., Kuwahara, N., Nakata, M. and Kaneko, M. *Macromolecules* 1975, **8**, 799
- 16 Kato, T., Miyaso, K., Noda, I., Fujimoto, T. and Nagasawa, M. *Macromolecules* 1970, **3**, 777
- 17 Bungert, B. *Diplomarbeit*, performed at University of California, Berkeley; deposited at Universität Dortmund, Fachbereich Chemietechnik, Arbeitsgruppe Physikalisch Chemische Verfahrenstechnik, 1992
- 18 Patterson, D., Delmas, G. and Somcynsky, T. *Polymer* 1967, **8**, 503
- 19 Goldwasser, D. J. and Williams, D. J. *Macromolecules* 1973, **6**, 353
- 20 Hino, T., Song, Y. and Prausnitz, J. M. *Macromolecules* 1994, **27**, 5681